MODIS Detached Coccolith Concentration

Algorithm Theoretical Basis Document

Version 4

Submitted by

Howard R. Gordon and William M. Balch[*]

University of Miami

Coral Gables, FL 33124

Under Contract Number NAS5-31363

April 30, 1999

[*]**Bigelow Laboratory for Ocean Sciences, Boothbay Harbor, ME**

TABLE OF CONTENTS

Preface

This algorithm theoretical basis document (ATBD) describes the present state of development of the algorithm for retrieving the concentration of detached coccoliths from the coccolithophore *E. huxleyi* and from other coccolithophore species. It replaces Version 0 which was submitted on July 30, 1993, Version 1 submitted February 28, 1994, and Version 2 submitted November 1, 1994. Version 1 was peer reviewed in the spring of 1994 and reviewer suggestions were incorporated into Version 2. Version 3 incorporates the progress of studies relevant to the algorithm since Version 2 (in particular, see Section 3.1.2) and was peer reviewed in November 1996. This Version 4 discusses recent validation work. The algorithm in its present form is being tested with SeaWiFS imagery of a major coccolithophore bloom in the Bering Sea. Experience gained with SeaWiFS imagery will be useful in assessing the performance of the algorithm when used with data from the Terra mission.

1.0 Introduction

Coccolithophores are small marine Prymnesiophyte phytoplankton which form external $CaCO_3$ scales (diameter $\sim$ a few μm and thickness 250 to 750 nm) called coccoliths. The coccoliths can form multiple layers and eventually detach. Coccolithophores are the largest source of calcium carbonate on earth [*Westbroek et al.*, 1985]. Of the coccolithophore species, *Emiliania huxleyi* is the most abundant, and its coccoliths can often be found from tropical to sub-arctic regions and further north into regions with water temperatures $< 0°$ C [*Heimdal*, 1983]. The distribution of *E. huxleyi* coccoliths in sediments matches the distribution of the overlying species in the water column [*McIntyre and Be*, 1967]. Dissolution of calcite depends on the depth of the calcite compensation depth. Approximately 20% of the biogenic carbonate is lost before accumulation in the sediments in regions such as the Sargasso Sea [*Fabry and Deuser*, 1990], while 97% is lost in the Arabian Sea [*Nair et al.*, 1989]. Even so, globally, calcium carbonate is responsible for about 75% of the deposition of carbon on the sea floor having a marine origin [*Groom and Holligan*, 1987; *Honjo*, 1986; *Honjo*, 1990], it and exceeds organic burial by a factor of seven. Thus, coccolith production is an important part of the biogenic carbon cycle.
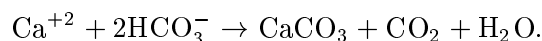
2.0 Overview and Background

The importance of coccolithophores to the overall particulate pool of phytoplankton had not been realized until the advent of remote sensing. Upwelling radiance measurements from the CZCS frequently showed large, mesoscale features in the temperate waters of both hemispheres. These features were sometimes characterized by complete saturation of band 3 (550 nm wavelength) of the CZCS. They were later attributed to intense light scattering by coccolithophores and associated coccoliths [*Holligan et al.*, 1983].

Perhaps the most intriguing aspect of coccolithophores concerns the frequency of their blooms. The archive of CZCS images shows alleged 100-200 km diameter coccolithophore blooms within temperate waters on an annual basis. Such blooms typically contain moderate to low chlorophyll concentrations so by inference, the organic carbon standing stock is low relative to the inorganic

carbon. Blooms have been observed by satellite off of Argentina (Podesta unpublished data), Northwest European Continental Shelf waters [*Groom and Holligan*, 1987; *Holligan et al.*, 1983], the Gulf of Maine[*Ackleson, Balch and Holligan*, 1989], Scotian Shelf (Balch unpublished), Southern California Bight [*Balch et al.*, 1989] and in the mid-Atlantic Bight and within warm-core rings [*Blackwelder*, 1984].

Apart from the inherent ecological interest in the development and fate of large-scale monospecific populations of phytoplankton, recent attention on the coccolithophores has focused on their role in global biogeochemical cycles. The flux of coccolith calcite to deep ocean water and sediments, which is known to have fluctuated in time [*Bramlette*, 1958; *McIntyre and McIntyre*, 1971], is recognized to be an important factor in determining the exchange of CO_2 between the oceans and the sediments [*Dymond and Lyle*, 1985; *Sarmiento, Toggweiler and Najjar*, 1988]. Over long time scales calcium carbonate is the major form in which carbon is buried in marine sediments [*Whitfield and Watson*, 1983], but in the short term the formation of calcite represents a source of CO_2 [*Paasche*, 1964] (but see *Sikes and Fabry* [1994]) due to the relationship

$$Ca^{+2} + 2HCO_3^- \rightarrow CaCO_3 + CO_2 + H_2O.$$

A further complication is that during warm climatic periods, including the present interglacial, rates of calcification in the oceans due to coccolithophores and other calcifying organisms[*Berger*, 1982; *Bramlette*, 1958; *Hay and Southam*, 1977] appear to be higher so that the above equation represents a potential positive feedback mechanism on levels of CO_2 in the atmosphere and, therefore, on global temperature.

These observations concerning coccolithophores: (1) their ubiquitous nature, (2) their possible role in climate, and (3) their intense scattering, make a global-scale study of their distribution an important application for MODIS imagery. We would ultimately like to estimate the rate at which $CaCO_3$ is formed by phytoplankton and look for long-term changes in that rate.

MODIS is ideal for such a study because of two unique characteristics: first its high radiometric sensitivity should, in principle, allow the detection of smaller quantities of coccoliths than CZCS; and second, the existence of the land bands on MODIS, e.g., band 3 and 4, with their high saturation radiance will enable study of very high concentrations of coccoliths that would saturate a typical ocean color instrument.

3.0 Algorithm Description

The algorithm for extracting the detached coccolith concentration from surface waters is based on the semianalytic model of ocean color of *Gordon et al.* [1988]. Briefly, the model relates the normalized water-leaving radiance ($[L_w]_N$), i.e., the radiance that would exit the ocean if the sun were at the zenith and the atmosphere were removed [*Gordon and Clark*, 1981], to the absorption and scattering properties of the constituents of the water using radiative transfer theory. The absorption and scattering properties are then related to the constituent concentrations through statistical analysis of direct measurements. Therefore, they represent oceanic- or regional-averaged relationships. The model is validated by comparison with a set of $[L_w]_N$'s [*Clark*, 1981] independent of the measurements used to establish the statistical relationships between constituents and optical properties.

3.1 Theoretical Description

In this section we first describe how the model is used to derive the detached coccolith algorithm. Next, we review the results of recent research, and discuss issues requiring further research. Finally, we discuss implementation of the algorithm, validation, and quality assurance.

3.1.1 Physics of the Algorithm

Unlike phytoplankton pigments, the presence of which decrease the radiance in the blue but increase it only slightly in the green, coccolithophore blooms tend to increase the radiance uniformly in both the blue and green [*Gordon et al.*, 1988]. Thus, their remote study requires an understanding of the actual water-leaving radiance rather than just radiance ratios as in the case of pigments [*Gordon and Morel*, 1983]. Furthermore the "flattening" of the reflectance spectrum of coccolithophore blooms implies that the standard pigment algorithms[*Gordon et al.*, 1983]will not provide correct pigment retrievals within the blooms. *Gordon et al.* [1988] have developed a prototype model for explaining the dependence of the water-leaving radiance on the concentration of constituents in Case 1 waters. This model provides the basis for extraction of the concentration of
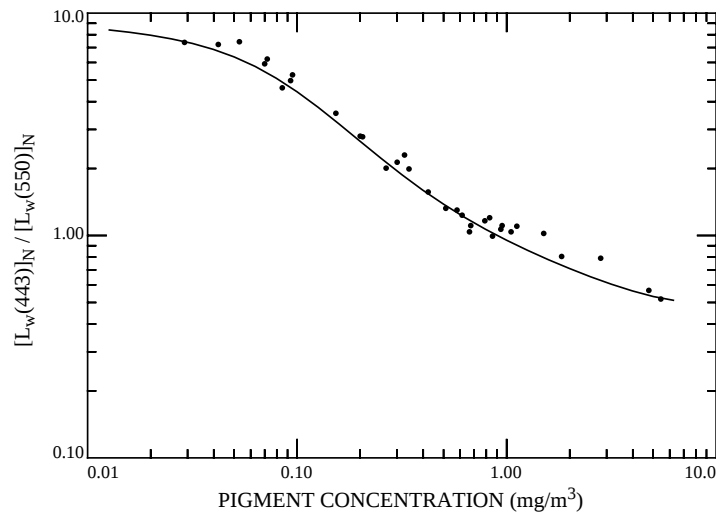
Figure 1. Variation in the $[L_w(440)]_N/[L_w(550)]_N$ with pigment concentration C. Points are Clark's[$Clark$, 1981] measurements and the solid line is the semi-analytic radiance model[$Gordon\ et\ al.$, 1988]in the absence of coccolithophores.
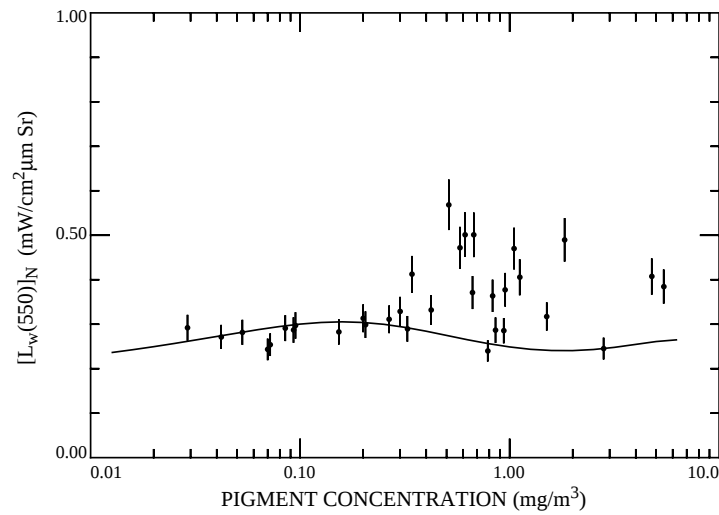
Figure 2. Variation in the $[L_w(550)]_N$ with pigment concentration C. Points are Clark's[$Clark$, 1981] measurements and the solid line is the semi-analytic radiance model[$Gordon\ et\ al.$, 1988]in the absence of coccolithophores.

the detached coccoliths of coccolithophores from the water-leaving radiance deduced from satellite imagery.

Briefly, the normalized water-leaving radiance is related to the absorption and scattering properties of the biogenic components of the water — phytoplankton and their associated detritus. The model is highly successful at explaining the dependence of the blue-green water-leaving radiance ratio on the pigment concentration (Figure 1). It is moderately successful at relating the actual radiances themselves to the pigment concentration. Figure 2 compares the computed and observed relationship between $[L_w(550)]_N$ and C. The "noise" in the relationship for $C > 0.3$ mg/m^3 is interpreted as being due to the natural variation in the backscattering of plankton and detritus. In the figure the plankton-detritus scattering parameter has been adjusted to provide the "best fit" for $C < 0.3$ mg/m^3. The resulting value is well within the range generally found for Case 1 waters [*Gordon and Morel*, 1983].

It is straightforward to introduce detached coccoliths from coccolithophores into the model by simply including their contribution to the backscattering. By direct measurement of detached
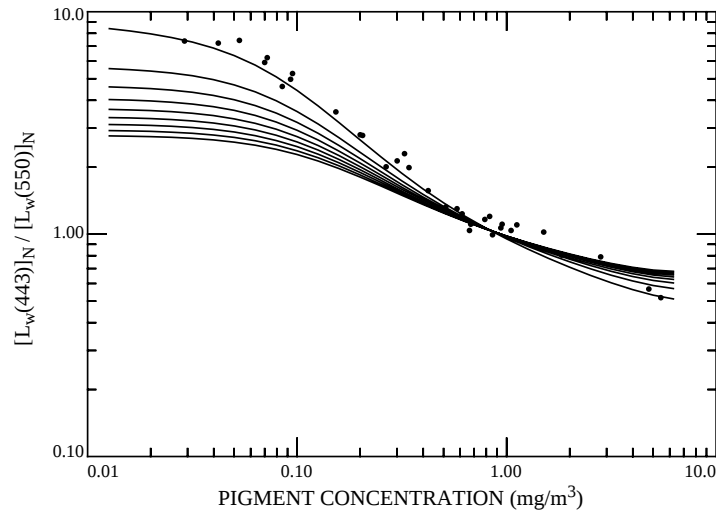

Figure 3. Variation in the $[L_w(440)]_N/[L_w(550)]_N$ with pigment concentration C. Points are Clark's[*Clark*, 1981] measurements and the solid line is the semi-analytic radiance model [*Gordon et al.*, 1988]. The coccolith concentration varies from 0 to 200×10^9 coccoliths/m^3. The higher coccolith concentrations yield the "flatter" curves.

coccoliths in the Gulf of Maine, *Balch et al.* [1991] have shown that at 436 and 546 nm the backscattering coefficient $b_b(\lambda)$ of the detached coccoliths can be approximated by

$$b_b(\lambda) = A(\lambda)C_{cc}, \tag{1}$$

where C_{cc} is the concentration of detached coccoliths, $A(436) \approx 1.5 \times 10^{-13}$ m^2 coccoliths^{-1}, and $A(546) \approx 1.1 \times 10^{-13}$ m^2 coccoliths^{-1}. Based on these measurements we approximate the spectral variation of $b_b(\lambda)$ by

$$b_b(\lambda) \propto \lambda^{-1.35}. \tag{2}$$

This relationship has been confirmed by *Voss, Balch and Kilpatrick* [1998].

Figures 3 and 4 provide the radiance ratio and $[L_w(550)]_N$ as a function of C and C_{cc} as derived from the radiance model. Examination of these figures suggest that C_{cc} can be retrieved from $[L_w(550)]_N$ to within a factor of two simply by assuming that $C = 0.5$ mg/m^3, e.g., if $C = 0.5$ mg/m^3 and $C_{cc} = 10^5$ ml^{-1}, then assuming $C \approx 0.01$ mg/m^3 yields $C_{cc} \approx 65 \times 10^9$ coccoliths/m^3, while assuming $C \approx 6$ mg/m^3 yields $C_{cc} \approx 200 \times 10^9$ coccoliths/m^3. However, given an estimate of C_{cc}, we can use Figure 3 to provide a reasonable estimate of C, which in turn can be used to improve the estimate of C_{cc}. In fact, if we can isolate C into specific ranges, i.e., $C < 0.1$, $0.1 < C < 0.3$, $0.3 < C < 0.5$, $0.5 < C < 1$, $1 < C < 2$, and $C > 2$ mg/m^3, which Figure 3 suggests can be done with little influence from the coccolith scattering, C_{cc} can be estimated with an error $\sim$ 10-20%. Note, however, that the basic relationship between b_b and C_{cc}, i.e., Eq. (1) is not established to this accuracy. The procedure is simplified by trying to estimate C and C_{cc} simultaneously from $[L_w(440)]_N$ and $[L_w(550)]_N$. A graphical scheme for effecting this based on the semi-analytical radiance model is provided in Figure 5. Examination of Figure 4 suggests that the natural variation in phytoplankton backscattering for $C < 10$ mg/m^3 corresponds to a change in C_{cc} from 0 to 25×10^9 coccoliths/m^3. Thus given accurate values of $[L_w(\lambda)]_N$, there will always be a 25×10^9 coccoliths/m^3 uncertainty in C_{cc} with a CZCS-type instrument. Figure 5 suggests that the sensitivity of the radiances to C_{cc} falls by about a factor of two from high C to low C. Note that Figure 5 provides a *simultaneous* method for deriving *both* C_{cc} and C in coccolithophore blooms; however, the sensitivity to C for $C > 2$ mg/m^3 is very poor. It forms the basis of the coccolith algorithm.
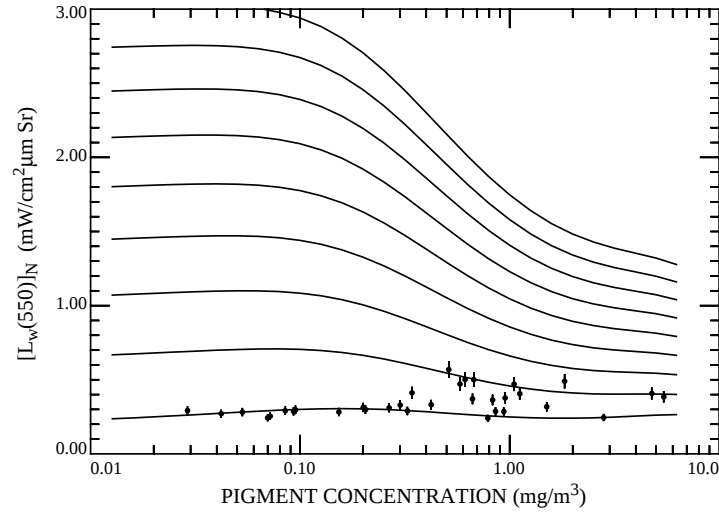
Figure 4. Variation in the $[L_w(550)]_N$ with pigment concentration C and the concentration of detached coccoliths. Points are Clark's[$Clark$, 1981] measurements and the solid line is the semi-analytic radiance model [$Gordon$ et $al.$, 1988]. The coccolith concentration varies from 0 to 200×10^9 coccoliths/m^3 from bottom to top.
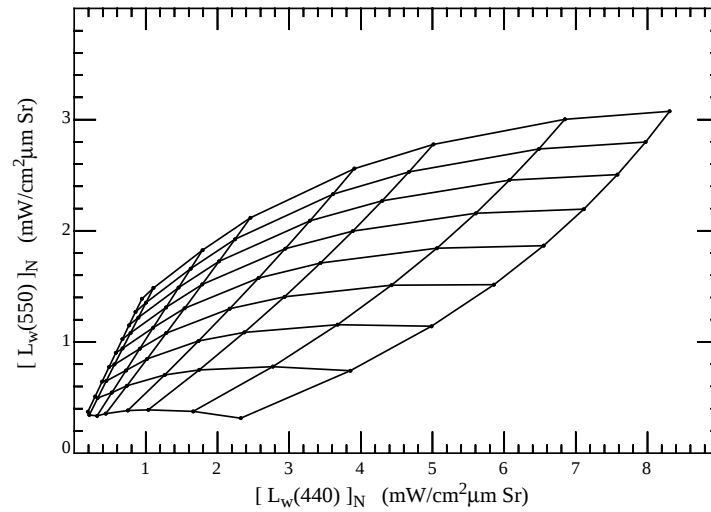

Figure 5. $[L_w(550)]_N$ as a function of $[L_w(440)]_N$ for various combinations of C and C_{cc}. The less sloped lines are lines of constant C_{cc} ranging from 0 (bottom) to 200×10^9 coccoliths/m^3 (top) in steps of 25×10^9 coccoliths/m^3. The more sloped lines are lines of constant C. The C-values are 0.03, 0.1, 0.2, 0.3, 0.6, 1, 2, and 6 mg/m^3 from right to left.

3.1.2 Recent Advances and Issues Requiring Further Study

The algorithm is based on Eqs. (1) and (2), which represents the scattering by detached coccoliths in the Gulf of Maine. It is a theoretical construct based on a model that appears to be valid for U.S. coastal and oceanic waters. At best the results are specific to this species and to the detached coccoliths. The yield of the algorithm (Figure 5) is the detached coccolith concentration (number m^{-3}), and more recently, CaCO$_3$ concentration.

We need to understand the wider applicability of the present algorithm. Due to the difficulty of sampling in coccolithophore blooms (their existence was rarely described prior to satellite imagery), we have focussed on understanding the scattering properties of various species of coccolithophores and detached coccoliths by using mostly cultures. It was found that the backscattering normalized to calcite concentration (calcite-specific backscatter $(b_b)^*_{Ca}$) showed significantly less variation than the backscattering normalized to coccolith concentration, suggesting the possibility of a more-appropriate calcite retrieval algorithm rather than an algorithm that retrieves the number density of detached coccoliths. Also, the intense bloom that we were able to sample showed that the calcite-specific backscatter $(b_b)^*_{Ca}$ of the natural bloom fell between the $(b_b)^*_{Ca}$ for detached coccoliths and the $(b_b)^*_{Ca}$ for a mixture of intact plated cells and detached coccoliths. This section highlights some of these studies. However, due to the paucity of the natural blooms that have occurred in the last several years, the range of variability of $(b_b)^*_{Ca}$ remains to be determined.

3.1.2.1 Review of Coccolith Backscattering

We have made considerable progress in understanding how the algorithm can be applied to coccoliths produced by open ocean blooms of *E. huxleyi* and by other commonly found species of coccolithophores. Most importantly for biogeochemical models, we have modified the algorithm to yield the suspended calcite concentration of the water directly, rather than the concentration of coccoliths. We originally ignored the scattering by intact cells, both naked and plated; however, *Bricaud, Morel and Prieur* [1983] have shown that the *E. huxleyi* cells themselves are very strong scatterers. Thus, we needed to know the relative importance of the effect of plated cells, naked cells, and coccoliths on $[L_w(\lambda)]_N$, as cells misinterpreted as detached coccoliths may be a potential source of error. The work of *Voss, Balch and Kilpatrick* [1998] addressed this discrimination. Experiments were performed to determine the coccolith-specific scattering coefficients in culture as well as the

effects of growth-phase on coccolith morphology and light scattering [*Balch et al.*, 1999; *Fritz*, 1997]. Preliminary data has shown that the detachment rate of coccoliths from cells generally is the same as the growth rate. Thus, by documenting the rate of increase of detached coccoliths in the field, growth rate information about coccolithophores may also be acquired. To our knowledge, this is a unique opportunity for understanding the growth of an important primary producer based on satellite measurements. We have performed important preliminary experiments to measure the calcite-dependent scattering of coccoliths from various species [*Balch et al.*, 1999]. Basically, a flow cytometer was used to sort individual coccoliths and plated cells into filtered seawater. Then the volume scattering function was measured. We found that for seven species of calcifying algae, the coccolith-specific backscattering coefficient, b_b^*, the measured backscattering coefficient b_b divided by the concentration of coccoliths, varied by a factor of about 70 (Figure 6). We hypothesized that if backscattering coefficients of calcite covered cells were calculated per unit mass calcite, then the backscattering coefficient would be much less variable, regardless of species. We found in earlier experiments with bulk cultures, that calcite-specific b_b^* of plated coccolithophores had low variance, only varying a factor of 3 across the species examined (Figure 7). The limitation of these experiments were that we only could use size fractionated cells from bulk cultures (which contained mixtures of plated cells, naked cells, and detached coccoliths), and those plated cells obviously contained both particulate inorganic carbon (as calcite) and particulate organic carbon; they did not contain pure calcite. Moreover, the flow cytometer still could not sort non-fluorescing, scattering coccoliths, free from organic matter. This was because we had no distinct "tag" that we could use to separate coccoliths from other non-fluorescent detritus. The problem of mixing organic and inorganic carbon became particularly acute in our measurements of the calcifying dinoflagellate *Thoracosphaera sp.*, in which the presence of cellular protoplasm in the calcite thecae significantly altered the scattering coefficient of the whole particle. The issue that we faced in subsequent experiments was to measure the calcite-specific backscattering coefficient for pure biogenic calcite particles, free of cells. Therefore, we set out to design the definitive experiment in which we used a flow cytometer to sort pure coccolith suspensions, after which light scattering was examined. This required major enhancements of our analytical abilities, both in flow cytometry and in calcite detection.
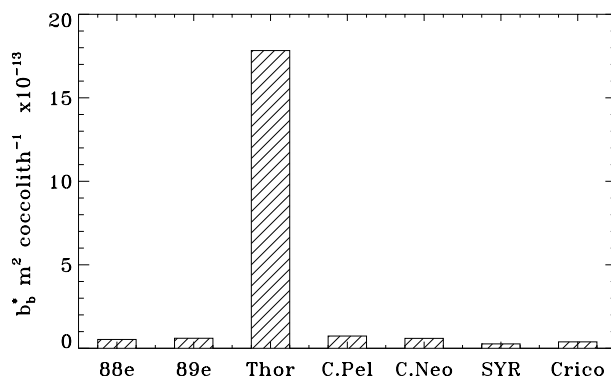
Figure 6. Total backscatter per calcite particle at 546 nm $[b_b^*$; m^2 (Calcite particle)$^{-1}]$ for several species of calicifying algae. In order from left to right: *Emiliania huxleyi*, strain 88e; *Emiliania huxleyi*, strain 89e; *Thoracosphaera sp.*; *Coccolithus pelagicus*; *Coccolithus neohelis*; *Syracosphaera sp.*; and *Cricosphaera sp.* Total variability is about 70X between the various species.
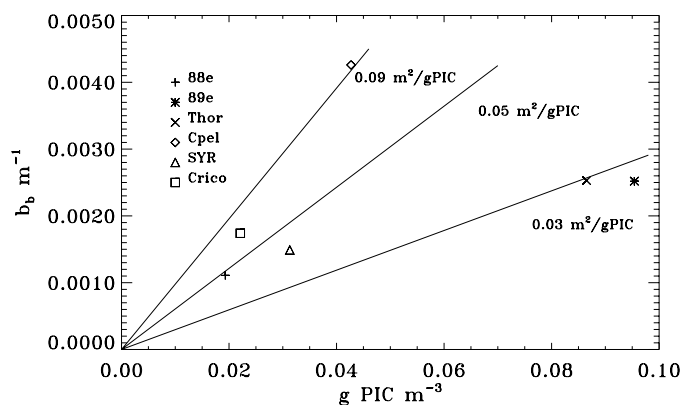
Figure 7. Acid labile backscatter at 546 nm $[b_b$; m$^{-1}]$ for several species of calicifying algae shown in Figure 6. PIC is Calcite carbon. Symbols are as follows: + *Emiliania huxleyi*, strain 88e; * *Emiliania huxleyi*, strain 89e; × *Thoracosphaera sp.*; ◇ *Coccolithus pelagicus*; △ *Syracosphaera sp.*; and □ *Cricosphaera sp.* Slopes of the three lines represent the total variation in the calcite-specific backscatter which is about 3X. Multiplication of the slopes by 12 gives the specific scattering coefficient in units of m^2/mole, i.e., the values on the figure correspond to 1.08, 0.60, and 0.36 m^2/mole. Note that these cultures are a mixture of coccoliths and plated cells of unknown relative concentrations

3.1.2.2 Recent Laboratory Experiments

We ran a series of flow cytometer experiments at Bigelow Laboratory with the goal of sorting individual coccoliths with the flow cytometer, to measure the volume scattering properties of the sorts, then to measure the mass of calcite within the sort. Sorting of individual coccoliths is not trivial with the flow cytometer due to their small size and lack of autofluorescence, and it required careful tuning of the instrument so that we could sort coccoliths based on their birefringence (i.e., the ratio of horizontally- and vertically-polarized forward light scattering). Moreover, this work required much more precise measurements of calcium concentration, than heretofore made on these calcifying algal species. This was particularly difficult when one considers that seawater (and flow cytometer sheath fluid) has Ca^{++} concentrations in excess of 10 mM. Fortunately, we have access to a graphite furnace atomic absorption spectrometer, with three orders of magnitude more sensitivity (50 pg Ca ml^{-1}) than flame atomic absorption. The instrument, a Perkin Elmer Model 5100PC, belongs to Dr. Larry Mayer at the Darling Center, University of Maine (Walpole, ME). As an example of the experiments, we sorted 100,000 coccoliths of *Emiliania huxleyi* (2 μm diameter) with the flow cytometer. This translated to 25 ng C or 83 ng Ca, which, in a 5 mL final volume, gave a concentration of 16.6 ng Ca ml^{-1} (still sufficient to give a signal to noise ratio > 300 on the graphite furnace atomic absorption spectrometer).

Species of calcifying algae (both coccolithophores and *Thoracosphaera heimii*, the calcifying dinoflagellate) were purchased from the Provasoli-Guillard Culture Collection (at Bigelow Laboratory), and grown in K media. Cultures were kept in the temperature-controlled rooms at Bigelow on a 14h:10h light:dark cycle and harvested in logarithmic growth phase for sorting with the EPICS V flow cytometer with multi-parameter data acquisition. Calcite particles then were sorted based on their birefringence under the laser light. Polarizing filters were placed, at right angles, on the two forward-angle scatter detectors of the flow cytometer[*Olson, Zettler and Anderson*, 1989]. Olson showed that the ratio of horizontally to vertically polarized forward light scatter was about 3 for calcite particles and 1 for all other particle types (we have found a ratio closer to 12 for coccoliths using the Bigelow Laboratory flow cytometer). This proved highly effective for discriminating and sorting calcite particles. Two species, *Syracosphaera sp.* and *Coccolithus pelagicus* grew in clumps which caused problems in sorting individual coccoliths. The other three species, *E. huxleyi* (clone 89E), *Cricosphaera sp.*, and *Thoracosphaera sp.* were adequate for our experiments.

The results showed that, indeed, the coccolith-specific backscattering coefficients were highly variable as indicated by the differences in slopes of the lines in Figure 8. All comparisons of b_b particulate versus the concentration of Ca are shown in Figure 9 and demonstrate much less variance than the coccolith-specific values (Figure 6). Backscattering coefficients of 6 calcifying algal species, as well as field-derived calcite particles, were normalized to the concentration of suspended calcite $(b_b)^*_{Ca}$ [m^2 (mol Ca)$^{-1}$) to see whether the the values of $(b_b)^*_{Ca}$ were less variable than $(b_b)^*_{partic}$. The least squares fit line (at 632 nm; forced through zero; standard errors also given in parentheses) was: $(b_b)^*_{Ca} = (6.95 \pm 0.492) \times [CaCO_3]/V$, where $[CaCO_3]/V$ is the molar concentration of calcium carbonate ($r^2 = 0.57$; $F = 34.1$; Degrees of freedom = 26; residual sums of squares = 4.69×10^{-4}; coefficient of variation of slope in Figure 9 = 38%; this varied slightly depending on whether or not the regression intercept was driven through zero).
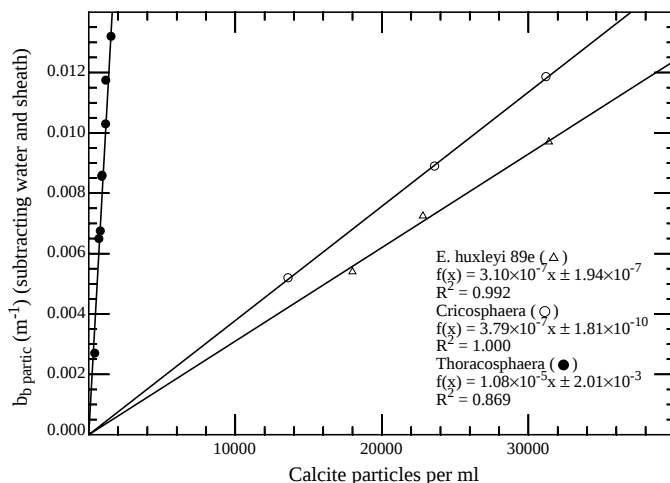
Figure 8. Particulate backscattering versus numbers of calcite particles for *E. huxleyi* coccoliths (open triangles), *Cricosphaera* coccoliths (closed circles) and empty thecae of *Thoracosphaera sp.* (open circles). Concentrations of calcite particles based on light microscope counts.

The calcite-specific $(b_b)^*_{Ca}$ based on pure sorts of coccoliths was about 6–15 times higher than the values based on cultures. Our previous results on cultures, which contained plated cells, naked cells, and detached coccoliths, gave calcite-specific b_b^* values between 0.36 and 1.08 m^2/mole (Figure 7). Field values obtained during a coccolithophore bloom off Iceland were between the values for pure detached coccolith sorts and the cultures. This comparison is provided in Figure 10, with the

bloom yielding a calcite-specific b_b^* of 1.36 m^2/mole. The presence of absorbing organic matter
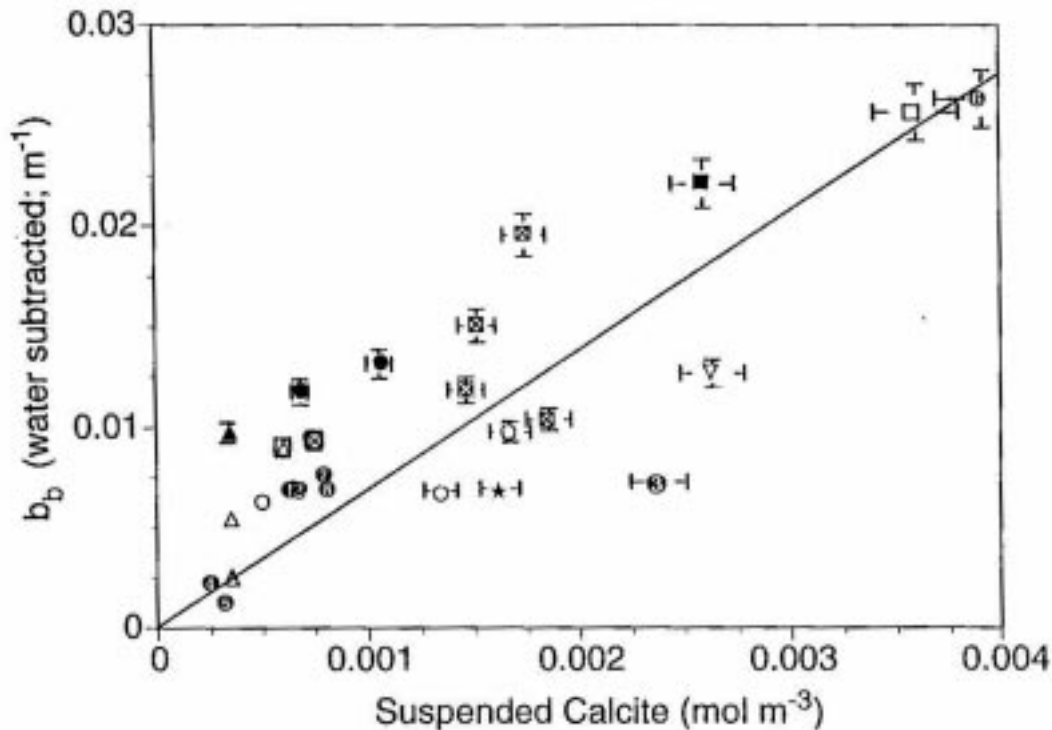
Figure 9. Backscattering vs. calcite concentration (mol m^{-3}) for bulk culture samples (open symbols) with all cells removed by filtration leaving just detached coccoliths and flow cytometer sorts (solid symbols) of detached coccoliths. These data were collected using several experimental designs [*Balch et al.*, 1999]. Measurements of field particles are denoted with black numbered circles. At typical coccolith concentrations in sea water, field samples had to be filter concentrated before running through the flow cytometer. In most cases, samples from several stations were combined to have sufficient numbers of particles for sorting. Error bars represent one standard deviation. When error bars are not shown, they are smaller than the symbol on the plot. See *Balch et al.* [1999] for the locations of the field stations. Species denoted as follows: E. huxleyi clone 88E = stars; E. huxleyi clone 89E = triangles; Thoracosphaerasp. = circles; Pleurochrysis sp. = squares; S. elongata = inverted triangles; and C. roscoffensis = crosses. Field sample results denoted with numbers: 1 = Arabian Sea Stn 10 small; 2 = Arabian Sea Stn 10 large; 3 = Arabian Sea Stn 14-17 small; 4 = Arabian Sea Stn 1 and 3 small; 5 = Arabian Sea Stn 1 and 3 large, 6 = CoBop Stn 1, 7 = Arabian Sea Stns 18, 21, 30, 32 small; 8 = Arabian Sea Stns 18, 21, 30, 32 large. The results show that the two different methods of separating detached coccoliths from cells provide comparable results, and also that the backscattering by detached coccoliths of different cultured species and detached coccoliths of species found in natural waters are similar when normalized to the calcite concentration.

obviously reduces the calcite-specific backscattering, although the mechanism is not known. The

measurements of *Voss, Balch and Kilpatrick* [1998] and *Balch et al.* [1999] clearly show the plated cells backscatter much more strongly on a per particle basis than detached coccoliths; however, the backscattering of plated cells on a per calcite basis is not known because the number of coccoliths per plated cell has not been measured in the experiments, and can be highly variable. Such observations serve to emphasize the differences between pure coccolith suspensions and natural conditions. The variability of calcite-specific b_b^* in natural waters under bloom conditions is a subject that will be a major focus of our post-launch effort.
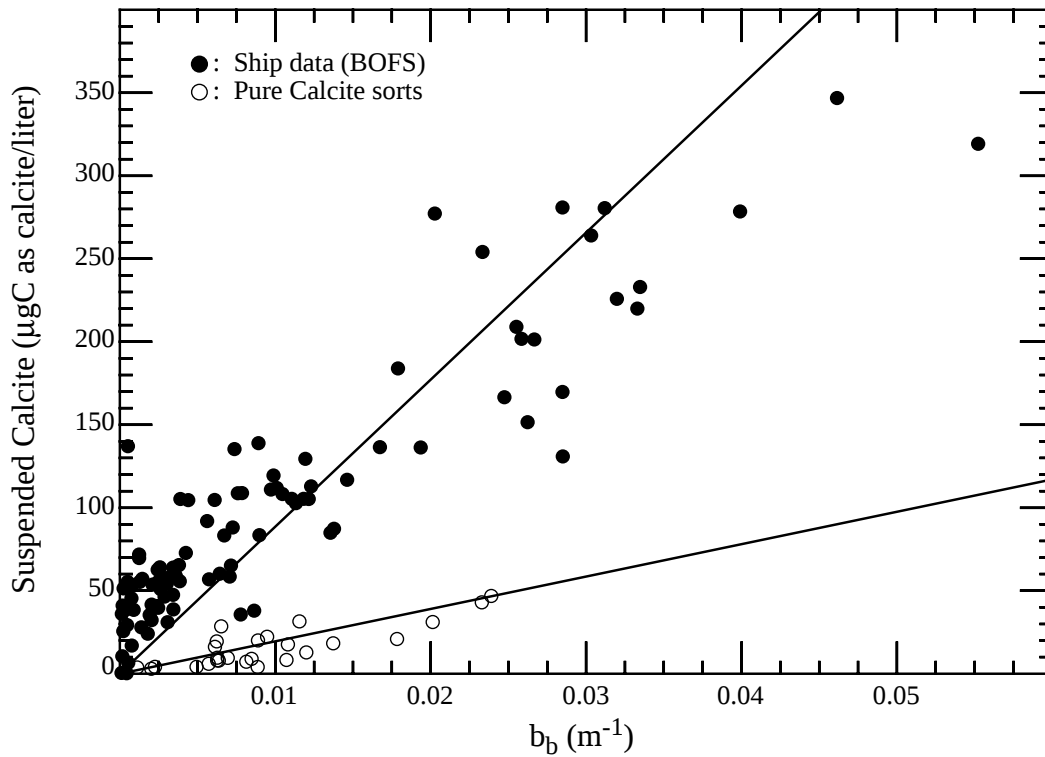
Figure 10. Comparison between the calcite-specific $(b_b)_{Ca}^*$ and the calcite concentration for pure sorts of calcite detached coccoliths and a natural (intense) coccolithophore bloom off Iceland. The values of $(b_b^*)_{Ca}$ at 550 nm were 1.36 m^2/mole for the bloom and 6.38 m^2/mole for the sorts.

Figure 9 also shows the results of the last phase of this work, in which we sorted natural calcite particles sampled from ships of opportunity from the world oceans. Included on this plot are data from cultured calcifying algae. Figure 11 provides electron micrographs of some of these species.
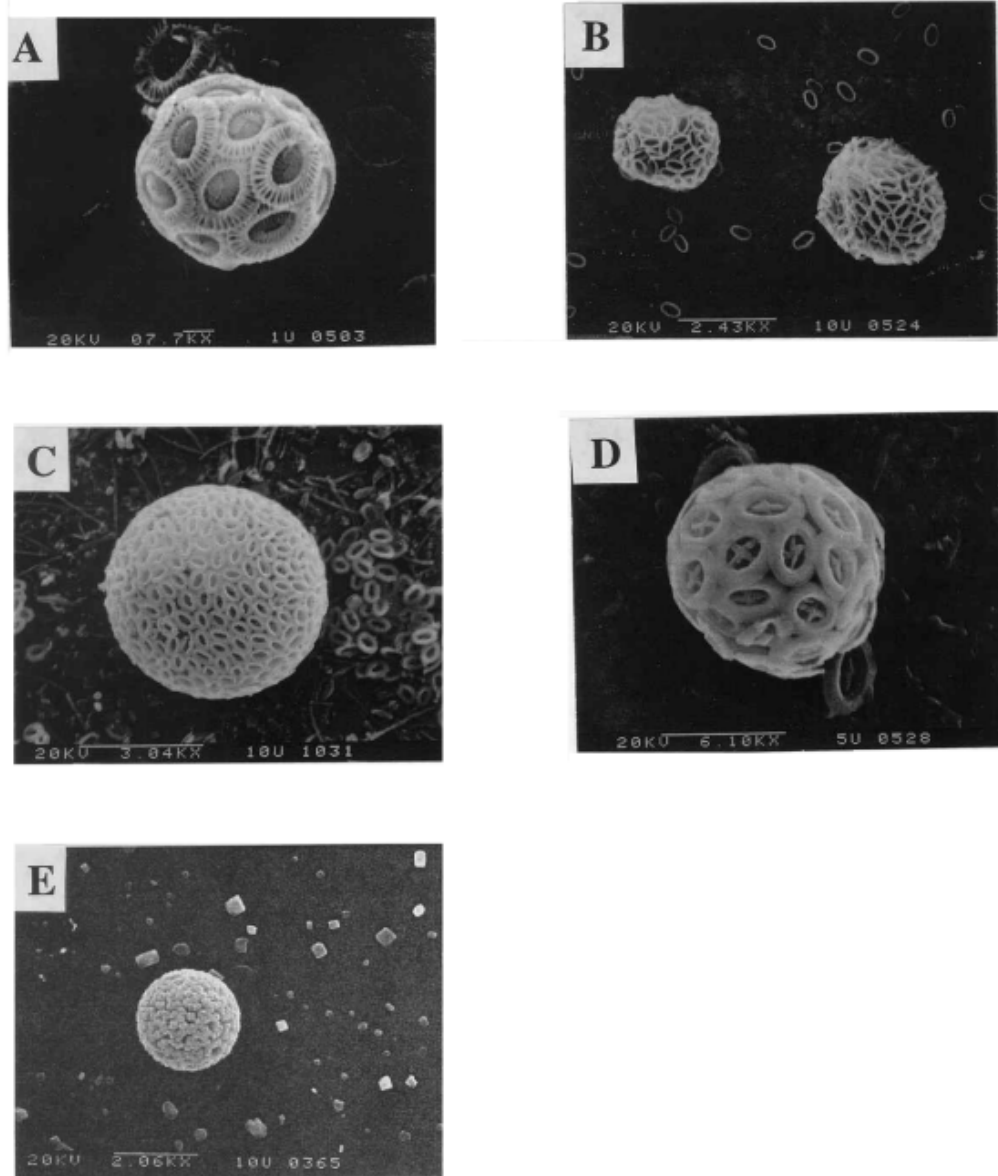
Figure 11. Scanning electron micrographs of calcifying algae used in these experiments. All species were coccolithophores except *Thoracosphaera sp.*, which was a dinoflagellate. The diameter (D) of each cell and coccolith respectively is: A) *E. huxleyi* clone 88E, D= 6.4 μm & 2.5 μm (scale bar = 1 μm); B) *C. roscoffensis*, D = 13.6 μm & 1.77 μm (scale bar = 10 μm); C) *Pleurochrysis sp.*, D = 18 μm & 1.6 μm (scale bar = 10 μm); D) *C. neohelis*, D = 18 μm & 2.1 μm (scale bar = 5 μm); E) *Thoracosphaera sp. thecae*, D = 11 μm (scale bar = 10 μm); Not shown: *E. huxleyi* clone 89E, D = 5.5 μm cell & 2.5 μm coccolith. *Syracosphaera sp.*, D = 18 μm cell & 2.1 μm coccolith.

These samples were sorted using the polarizing filters placed at right angles over the two forward-angle scatter detectors of the flow cytometer. This provided a more representative estimate of the backscattering coefficient for naturally-occurring calcite particles.

3.1.2.3 Recent Field Experiments

For obtaining field data on calcite-dependent backscattering, we have developed a second-generation underway scattering system. It uses a Wyatt Technologies laser-light scattering photometer equipped with a flow-through cell to measure volume scatter at 18 angles. Integration of this signal in the backward direction allows us to calculate backscattering in real time. The system also monitors chlorophyll fluorescence, pH, temperature, salinity and 18-channel volume scattering. A Global Positioning System was interfaced, as well. In response to ATBD reviewers' requests for above water radiance and irradiance measurements, we added a Satlantic SAS system in 1998. This consists of a radiance collector mounted on the bridge wing of the vessel, aimed at $\sim30°$ from nadir, forward of the ship's wake. The sensor is measuring radiance at the SeaWiFS wavelengths. A downwelling irradiance sensor (for the same wavelengths) is mounted on the upper compass deck of the ship, away from superstructure and ship shadowing. These data are sent digitally to the laboratory container on the ferry's car deck. Underway L_w data are put through a rough filter to remove whitecaps, then averaged after each cruise.

We have now taken our flow-through light scattering detector to sea on many field campaigns and have a significant data base on the optical properties of calcite particles in the sea. Despite some very rough seas, the instrument has run without problem, and we recovered data first from four detailed transects across the Florida Straits for volume scattering (sampling at 400 per second, and averaging over 3-5 minute time intervals). These average volume scattering functions were used to calculate the backscattering coefficients on the same time scale. Given the velocity of the ship, this translated to horizontal resolution of about 900 m. (This can be shortened to 300 m resolution with no problem). While returning to Miami, we scaled 3 orders of magnitude in b_b, most of it resulting from calcite particles being resuspended and sloughing off the carbonate banks of the SE Florida shelf. Such high concentrations of suspended calcite are similar to the most dense coccolithophore blooms that we have ever visited; this raises interesting questions about the importance of suspended calcite to overall light scattering in Case 2 waters near carbonate banks.

We also have taken the system to the Indian Ocean to make MODIS pre-launch optical measurements. We connected the system to the underway flow-through system aboard the R/V Thomas Thompson in the Arabian Sea for a 35 day cruise during the intermonsoon period. The instrument ran virtually flawlessly, and we collected continuous data of total backscattering and calcite-dependent backscattering over the 3500 km cruise track. Interestingly, we demonstrated that consistently 10-30% of the total backscattering in the Arabian Sea was acid-labile (i.e., originated from calcite). The instrument also logged statistics of the backscattering events every 4 minutes of the trip. The data showed that various water masses could be characterized by well-defined scattering statistics (e.g., a striking relationship between the standard deviation of the scattering events, and the average backscattering value was found, suggesting a changing role of rare, large scatterers in certain water masses over the cruise track).

Relatively speaking, the Arabian Sea is not a region known for meso-scale coccolithophore blooms. In March and June of 1996, we had an opportunity to take the flow-through instrument into the Gulf of Maine where the coccolithophore, *Emiliania huxleyi* forms large blooms. As expected, calcite-dependent backscattering was low in March, but it was still measurable. In June 1995, we ran 2000 miles of transect in the Gulf of Maine with our flow-through light scattering photometer and may have observed the early stages of coccolithophore bloom development in Wilkinson Basin. Acid-labile scatter dropped over Georges Bank, and increased in the Northeast Channel, similar to previous blooms that we have observed. The observations are consistent with the calcite being produced in the more stable Wilkinson Basin with subsequent advection around the NE flank of Georges Bank. We performed another series of cruises in the Gulf of Maine cruise at the end of October, 1995, June 1996, November 1996, June 1997, November 1997 and June 1998. Each of these trips covered 1500 - 1800 nautical miles, with our optical underway system in almost constant operation. The data have all been submitted to SeaBASS.

Unfortunately, there have been no intense coccolithophore blooms in the Gulf of Maine (a usually reliable source) during any of these field experiments (the last major bloom was in 1991). We have routinely found coccolith concentrations of about 5000 per ml, enough to see an optical impact but still only about 1% of the coccolith concentration in a bloom. For the intense bloom sampling needed to understand the natural variability of $(b_b)^*_{ca}$ we have devised a strategy that allows rapid access to the Gulf by utilizing a ferry boat that makes daily crossings. Sampling began from the M/S Scotia Prince in September 1998, as part of the SIMBIOS project. We

added significant coccolithophore activities in support of our MODIS studies (coccolith counts, scattering due to coccoliths, suspended calcite measurements, etc.). We are still processing the atomic absorption samples for suspended calcite concentrations. So far a total of eleven ferry campaigns have been completed. The use of this ferry will be central to validation of the MODIS calcite retrievals.

3.1.2.4 Issues Requiring Further Study

The results of the field and laboratory experiments show that $(b_b)^*_{Ca}$ assumed significantly different values for cultures with plated cells (0.36 to 1.08 m^2/mole), for detached coccoliths ($\sim$6.5 m^2/mole), and for an intense oceanic bloom ($\sim$1.36 m^2/mole). The value of $(b_b)^*_{Ca}$ for plated cells will depend on the number of *attached* coccoliths, which may be highly variable. The ratio of detached coccoliths to plated cells is also highly variable. Thus, there are good reasons to expect significant variability in $(b_b)^*_{Ca}$, i.e., there is a potential for a very high variance in this quantity, and, as we have sampled only one intense oceanic bloom, the magnitude of this variance is unknown. In the initial implementation of the algorithm, we will use $(b_b)^*_{Ca}$ =1.36 m^2/mole at 550 nm, the value measured in the one intense North Atlantic bloom sampled in 1999.

We believe that establishing realistic limits for the variation of $(b_b)^*_{Ca}$ from bloom to bloom is paramount for making MODIS coccolith/calcite data useful. However, this is a very difficult task because for the most part the existence of intense coccolithophore blooms can only be confirmed by satellite imagery, and the long lead time for mounting a ship experiment precludes sampling them, i.e., due to their transient nature they are over by the time one can put a ship in the proper location. The Gulf of Maine ferry boat experiments provides an inexpensive alternative that has a high potential for success, as the ship track has traversed intense blooms in the past. These ferry-boat cruises will continue into the post-launch era, with the goal of validating the algorithm and establishing the natural variability of $(b_b)^*_{Ca}$. On these cruises we will measure $[L_w]_N$, calcite concentration, and $(b_b)^*_{Ca}$, make cell and coccolith counts, and estimate the number of coccoliths per plated cell.

In addition, we will participate in several other (more traditional) Gulf of Maine cruises in the post-launch era, and use MODIS and SeaWiFS data to steer the ship to offshore coccolithophore blooms.

3.1.3 Mathematical Description

The algorithm as presently configured consists of a set of lookup tables providing information similar to Figure 5. However, there may have to be sets that are specific to particular regions (because of speciation variations and/or variations in the ratio of detached coccoliths to plated cells) and to latitude belts. *Mitchell* [1992] has shown that the chlorophyll-specific absorption coefficient of particulate matter in the polar regions is significantly lower than in the temperate oceans. Thus, application of the algorithm to polar regions would require the *Gordon et al.* [1988] model be modified to reflect this fact. In fact, there may be a range of chlorophyll-specific absorption coefficients [*Carder et al.*, 1991] requiring region-specific algorithms. Also, to the extent that a single species of coccolithophore dominates intense blooms in certain regions, e.g., *E. huxleyi* in the North Atlantic or *Umbilicosphaera sibogae* in the California Current [*Balch et al.*, 1989], it may be necessary to have species-dependent algorithms for particular regions and times. This would require species-dependent versions of Eqs. (1) and (2); however, in the case of the more-meaningful calcite concentration, the species-dependent variations are significantly smaller.

3.1.4 Uncertainty Estimates

Since the algorithm uses absolute values of the water-leaving radiances, it is more susceptible to errors in atmospheric correction than algorithms employing radiance ratios. Thus, atmospheric correction can be an important source of error over and above the inherent error in the algorithm due to natural variability. It is possible to understand the effects atmospheric correction errors on C_{cc} in a simple manner. If the atmospheric correction is in error by ± 0.001 in reflectance ($\pi L/F_0 \cos \theta_0$, where L is the radiance, F_0 is the extraterrestrial solar irradiance, and θ_0 is the solar zenith angle), the error in the radiance will be approximately ± 0.06 mW/cm$^2\mu$m Sr in each band for small θ_0. From this we can use Figure 5 to ascertain that the error due to atmospheric correction will be small $\Delta C_{cc} < \pm 5 \times 10^9$ coccoliths/m^3 for low C and $\sim \pm 10 \times 10^9$ to $\pm 15 \times 10^9$ coccoliths/m^3 for $C \sim 2$ mg/m^3. However, errors in sensor calibration can also cause errors in the recovered water-leaving radiance. (See *MODIS Normalized Water-leaving Radiance Algorithm Theoretical Basis Document*, by H.R. Gordon, for a discussion, with numerical examples, of the influence of sensor calibration errors on $[L_w]_N$.) Given a scenario yielding an estimated error in $[L_w]_N$, Figure 5 can be used to estimate the corresponding error in C_{cc} and C in a trivial way.

Another potential source of error is derived from the fact that the atmospheric correction algorithm assumes that $[L_w(\lambda)]_N = 0$ for $\lambda = 765$ and 865 nm, i.e., in the near infrared (NIR). For sufficiently high coccolith concentrations this will be violated which will degrade the atmospheric correction and therefore the retrieval of $[L_w(\lambda)]_N$ in the blue and green, introducing more uncertainty in C_{cc}. In order to estimate the seriousness of this problem, scattering (or normalized water-leaving radiance) data is required in the NIR. Currently we measure scattering at 680nm based on attenuation and absorption measurements with an AC-9. Moreover, in an effort to further constrain wavelength variability in backscattering, we have installed a Hobie Labs "Hydroscat-2", which measures backscattering at 438 and 683 nm. Since our Wyatt Technologies instrument measures backscattering at 513nm, we will now be able to estimate the wavelength dependence of total scattering and backscattering in the red. Note, the SAS system is also measuring red water-leaving radiance, as well. Without these new measurements, if one assumes that Eq. (2) is valid into the NIR, then for $C_{cc} = 100 \times 10^9$ coccoliths/m^3, the error ($bias$) introduced into $[L_w(\lambda)]_N$ in the blue-green is about –0.2 mW/cm$^2\mu$m Sr, or about one small scale division on the axes of Figure 5. We hope to lessen this error even more with the new instrumentation.

However, thus far our field and laboratory studies suggest that the largest potential error is the natural variability of $(b_b)^*_{Ca}$. At this time, it is not possible to comment on the magnitude of this variability.

3.2 Practical Considerations

We believe that the lookup table approach described above is optimum, and this is our working hypothesis. Significant modification or an entirely different approach may be required for the final algorithm, e.g., it might be necessary to analytically derive $b'_{cc}(\lambda)$ using the radiance model and then derive C_{cc} using Eq. (1). It is too early to speculate on some portions of the individual subsections below and parts are occasionally marked "TBD" (To Be Determined). Please note that those that are not marked TBD are not necessarily complete.

3.2.1 Validation

The validation of the C_{cc} and calcite concentration products will be effected by comparing simultaneous surface-based measurements and MODIS-derived values. This will be effected in the

pre-launch phase by utilizing ship data, i.e., comparing products derived from measurements of $[L_w]_N$ with those measured directly, as well as data from other ocean color sensors (SeaWiFS, OCTS, etc.) if available. In the post-launch phase, we shall participate in the MODIS Ocean Group validation effort (see Science Data Validation Plan, MODIS Oceans Group, available on World Wide Web at http://spso.gsfc.nasa.gov/validation/docs.html); however, we shall also carry out a validation effort specifically focused on coccoliths. For this, station locations will be chosen to provide a wide range of values; however, it will be centered on intense blooms, when available.

3.2.2 Quality Control and Diagnostics

If our assumptions are valid the algorithm can be expected to perform properly unless $[L_w(550)]_N$ is too small or too large (specific values are TBD). To insure that the algorithm results are of the highest quality, we will check the output relative to expected ranges. Output which falls beyond specified confidence limits will be flagged. For example, typical suspended calcite concentrations in the blue ocean fall between 0-1 μmol $CaCO_3$ per liter (a recent trip to the Equatorial Pacific showed concentrations of 0.2-0.3 over much of the Equatorial region). Values of 4 and 5 μmol $CaCO_3$ liter are easily found in the North Atlantic in summer but otherwise would be considered high. Blooms of coccolithophores will be characterized by calcite concentrations of 30-40 μmol $CaCO_3$ per liter. Higher suspended calcite concentrations in the sea have been observed before only in the rarest circumstances and output exceeding this concentration should be flagged (note, this is equivalent to *E. huxleyi* coccolith concentration of about 1.6 million coccoliths per ml!). At the minimum, this would probably allow us to differentiate when the high reflectance was due to coccolithophores or some other high-reflectance algae which is concentrated at the surface, e.g., *Trichodesmium*. Over the course of the mission, statistics will be developed with which algorithm results can be compared to previous determinations.

Another error that needs to be continuously monitored relates to the look-up table shown in Figure 5. Recall that as chlorophyll concentrations increase, the isopleths of chlorophyll are closer and closer together. In other words, a 10% error in $L_w(440)$ at low chlorophyll concentrations may only mean an absolute error of 0.01 μg Chl per liter, whereas the same error at low radiance values (high chlorophyll) will cause an error of 4 μg Chl per liter. The current version of the algorithm is least accurate at high chlorophyll concentrations, and values over about 5 μg Chl per liter should be flagged, whether calcite concentrations are high or low.

3.2.3 Exception Handling

Exceptions occasionally occur in a manner that prevents operation of the algorithm, e.g., missing data in bands the required bands near 440 and 550 nm, or data that fall outside the range of "reasonable" values. A series of flags indicate when the retrievals should not be attempted.

3.2.4 Data Dependencies

At this time, only $[L_w(443)]_N$ and $[L_w(550)]_N$ are expected to be needed; however, for quality assurance procedures, it will be necessary to have a low spatial resolution, global scale, time series of retrievals to signal the appearance of large unexpected changes in the output products. Assembly of this set will be effected along with similar sets for other MODIS ocean products collectively by the MODIS Oceans Group. The Gulf of Maine would be an ideal area for this time series due to our high frequency of visits.

3.2.5 Output Products

The output products will be C_{cc}, an estimate of the calcite concentration, C, a descriptor of the particular lookup table(s) used, and a quality measure based on the value of $[L_w(550)]_N$. If $[L_w(550)]_N$ is too low or too high (specific values are TBD), the algorithm may return poor results which will be indicated by the quality measure for each retrieved variable.

4.0 Assumptions and Constraints

In this section we describe the assumptions that have been made and how they may influence the resulting C_{cc} and C. We also provide scenarios for which the algorithm should not be used, and for which the returned value of C should be used in place of the standard ratio algorithm.

4.1 Assumptions

There are three main assumptions in this algorithm: (1) Eq. (1) is correct; (2) Eq. (2) is correct; and (3) the parameters in the radiance model are correct. Errors in these, and in particular the applicability of Eq. (1) and (2) on a global scale, will map to errors in the final product.

4.2 Constraints

The principle constraint is that the algorithm should only be used when $[L_w(550)]_N$ exceeds a given value (while we have had opportunities to test the algorithm in a few large blooms, the specific value is TBD). This value is above the range of the natural variation in $[L_w(550)]_N$ for a given C caused by variation in phytoplankton and associated detritus optical properties in the absence of coccoliths. Above this limit, the algorithm could be used to provide an estimate of C, which may be better than the estimate provided by the ratio algorithms in coccolithophore blooms. If $[L_w(550)]_N$ becomes too large (specific value is value TBD) the algorithm should not be used because atmospheric correction will be too strongly influenced by the presence of the coccoliths.

5.0 References

Ackleson, S. G., W. M. Balch and P. M. Holligan, White waters of the Gulf of Maine, *Oceanography*, *1*, 18–22, 1989.

Balch, W. M., D. T. Drapeau, T. L. Cucci, R. D. Vaillancourt, K. A. Kilpatrick and J. J. Fritz, Optical backscattering by calcifying algae-Separating the contribution by particulate inorganic and organic carbon fractions, *Jour. Geophys. Res.*, *104C*, 1541–1558, 1999 .

Balch, W. M., R. W. Eppley, M. R. Abbott and F. M. H. Reid, Bias in satellite-derived pigment measurements due to coccolithophorids and dinoflagellates, *Jour. Plankton Res.*, *11*, 575–581, 1989.

Balch, W. M., P. M. Holligan, S. G. Ackleson and K. J. Voss, Biological and optical properties of mesoscale coccolithophore blooms in the Gulf of Maine, *Limnology and Oceanography*, *34*, 629–643, 1991.

Berger, W. H., Deglacial CO_2 buildup: Constraints on the coral-reef model, *Palaeogeog. Palaeoclim. Palaeoecol.*, *40*, 235–253, 1982.

Blackwelder, P. W., Coccolithophore temporal and regional population dynamics and calcification in warmcore rings and NW Atlantic water, *EOS*, *65*, 912, 1984.

Bramlette, M. N., Significance of coccolithophorids in calcium carbonate deposition, *Bull. Geol. Soc. Am*, *69*, 121–126, 1958.

Bricaud, A., A. Morel and L. Prieur, Optical Efficiency Factors of Some Phytoplankters, *Limnology and Oceanography* , *28*, 816–832, 1983.

Carder, K. L., S. K. Hawes, K. S. Baker, R. C. Smith, P. G. Steward and B. G. Mitchell, Remote sensing model for discriminating marine gilvin from chlorophyll, *J. Geophys. Res.*, *96C*, 20,599–20,611, 1991.

Clark, D. K., Phytoplankton Algorithms for the Nimbus-7 CZCS, in *Oceanography from Space*, edited by J. R. F. Gower, pp. 227–238, Plenum Press, New York, NY, 1981.

Dymond, J. and M. Lyle, Flux comparisons between sediments and sediment traps in the eastern tropical Pacific: Implications for atmospheric CO_2 concentrations during the Pleistocene, *Limnology and Oceanography*, *30*, 699–712, 1985.

Fabry, V. J. and W. G. Deuser, Aragonite and Magnesian fluxes to the deep sea, *EOS*, *71*, 161, 1990.

Fritz, J. J., Growth dependence of coccolith detachment, carbon fixation, and other associated processes by the coccolithophore *Emiliania huxleyi*, 1997, Ph.D. thesis, University of Miami, 179p..

Gordon, H. R., O. B. Brown, R. H. Evans, J. W. Brown, R. C. Smith, K. S. Baker and D. K. Clark, A Semi-Analytic Radiance Model of Ocean Color, *Jour. Geophys. Res.*, *93D*, 10909–10924, 1988.

Gordon, H. R. and D. K. Clark, Clear water radiances for atmospheric correction of coastal zone color scanner imagery, *Applied Optics*, *20*, 4175–4180, 1981.

Gordon, H. R., D. K. Clark, J. W. Brown, O. B. Brown, R. H. Evans and W. W. Broenkow, Phytoplankton pigment concentrations in the Middle Atlantic Bight: comparison between ship determinations and Coastal Zone Color Scanner estimates, *Applied Optics*, *22*, 20–36, 1983.

Gordon, H. R. and A. Y. Morel, *Remote Assessment of Ocean Color for Interpretation of Satellite Visible Imagery: A Review*, Springer-Verlag, New York, 1983, 114 pp.

Groom, S. B. and P. M. Holligan, Remote sensing of coccoltihophore blooms, 1987, Proceedings XXVI COSPAR Meeting, Toulouse, France.

Hay, W. W. and J. R. Southam, Modulation of marine sedimentation by the continental shelves, in *The Fate of Fossil Fuel CO$_2$ in the Ocean*, edited by N. R. Anderson and A. Malahoff, pp. 569–604, Plenum Press, New York, 1977.

Heimdal, B. R., Phytoplankton and nutrients in the waters north-west of Spitsbergen in the autumn of 1979, *Jour. Plankton Res.*, *5*, 901–918, 1983.

Holligan, P. M., M. Viollier, D. S. Harbour, P. Camus and M. Champagne-Philippe, Satellite and Ship Studies of Coccolithophore Production Along the Continental Shelf Edge, *Nature*, *304*, 339–342, 1983.

Honjo, S., Oceanic particles and pelagic sedimentation in the western North Atlantic Ocean, in *The Geology of North America Vol. M, The Western North Atlantic Region*, edited by P. R. Vogt and B. E. Tucholke, pp. 469–478, Geological Society of America, 1986.

Honjo, S., Particle fluxes at 47°N and 34°N 20°W stations between April 3 to September 26, 1989, *EOS*, *71*, 81, 1990.

McIntyre, A. and A. W. H. Be, Modern Coccolithophorideae of the Atlantic Ocean — I.Placoliths and cyrtoliths, *Deep Sea Res.*, *14*, 561–597, 1967.

McIntyre, A. and RA. McIntyre, Coccolith concentrations and differential solution on oceanic sediments, in *The Micropaleontology of the Oceans*, edited by B. M. Funnel and W. R. Reidel, pp. 253–261, Cambridge Univ. Press, Cambridge, 1971.

Mitchell, B. G., Predictive bio-optical relationships for polar oceans and marginal ice zones., *J. Mar. Syst.*, *3*, 91–105, 1992.

Nair, R. R., V. Ittekkot, S. J. Monganini, V. Ramaswamy, B. Haake, E. T. Degens, B. N. Desai and S. Honjo, Increased particle flux to the deep ocean related to monsoons, *Nature*, *338*, 749–751, 1989.

Olson, R., E. R. Zettler and O. K. Anderson, Discrimination of eukaryotic phytoplankton cell types from light scatter and autofluorescence properties measured by flow cytometry, *Cytometry*, *10*, 636–643, 1989.

Paasche, E., A tracer study of the inorganic carbon uptake during coccolith formation and photosynthesis in the coccolithophorid Coccolithus huxleyi, *Physiologia Plantarum Supplementum*, *III*, 1–82, 1964.

Sarmiento, J. L., J. R. Toggweiler and R. Najjar, Ocean carbon-cycle dynamics and atmospheric pCO_2, *Phil. Trans. R. Soc. Lond. A*, *325*, 3–21, 1988.

Sikes, S. and V. Fabry, Photosynthesis, $CaCO_3$ deposition, coccolithophorids and the global carbon cycle, in *Photosynthetic carbon metabolism and regulation of atmospheric CO_2 and O_2*, edited by N. E. Tolbert and J. Preiss, Oxford University Press, London, 1994.

Voss, K., W. M. Balch and K. A. Kilpatrick, Scattering and attenuation properties of Emiliania huxleyi cells and their detached coccoliths, *Limnology and Oceanography*, *43*, 870–876, 1998.

Westbroek, P., E. W. D. V-D. Jong, P. V. der Wal, A. H. Borman and J. P. M. D. Vrind, Biopolymer-mediatedcalcium and manganese accumulation and biomineralization, *Geol. Mijnbouw*, *64*, 5–15, 1985.

Whitfield, M. and A. J. Watson, The influence of biomineralisation on the composition of seawater, in *Biomineralisation and Biological Metal Accumulation*, edited by P. Westbroek, E. W. de Jong and W. Reidel, pp. 57–72, 1983.